J. Math. Biol. (1998) 37: 341–371

Journal of Mathematical Biology

Modelling and analysis of time-lags in some basic patterns of cell proliferation

C. T. H. Baker,[1,*] G. A. Bocharov,[2] C. A. H. Paul,[1] F. A. Rihan[1]

[1] Mathematics Department, The Victoria University of Manchester, Manchester M13 9PL, England
[2] Institute of Numerical Mathematics, Russian Academy of Sciences, Moscow, Russia

Received: 15 September 1997/Revised version: 1 April 1998

Abstract. In this paper, we present a systematic approach for obtaining qualitatively and quantitatively correct mathematical models of some biological phenomena with time-lags. Features of our approach are the development of a hierarchy of related models and the estimation of parameter values, along with their non-linear biases and standard deviations, for sets of experimental data.

We demonstrate our method of solving parameter estimation problems for neutral delay differential equations by analyzing some models of cell growth that incorporate a time-lag in the cell division phase. We show that these models are more consistent with certain reported data than the classic exponential growth model. Although the exponential growth model provides estimates of some of the growth characteristics, such as the population-doubling time, the time-lag growth models can additionally provide estimates of: (i) the fraction of cells that are dividing, (ii) the rate of commitment of cells to cell division, (iii) the initial distribution of cells in the cell cycle, and (iv) the degree of synchronization of cells in the (initial) cell population.

Key words: Cell proliferation – Mathematical modelling – Time-lag – Neutral delay differential equation – Sensitivity analysis

1 Introduction

The bioscientific literature contains many reports of *in vitro* cell growth [5, 9–11, 14, 20, 23, 24, 36]. Some of these authors have attempted to

* Corresponding author. Email: cthbaker@ma.man.ac.uk. Fax +44 (0) 161 275 5819

provide insight into the cell proliferation processes using mathematical models based, in particular, on difference, ordinary differential and delay differential equations. In this paper, we compare some mathematical models of cell growth based on a hierarchy of differential equations, using data reported in [16], [22] and [24].

1.1 Cell proliferation

Whilst all cell growth has features in common [35], researchers seek to relate a culture's growth characteristics to those of the cells that compose the culture. Some of the characteristics they consider are: (i) the *culture-doubling time*, (ii) the *growth fraction*, (iii) the *average cell-division time* (the average time taken for a single cell to divide), (iv) *the rate of commitment of cells to cell division*, (v) the *initial distribution of cells in the cell cycle* (specified by a function), and (vi) the *degree of synchronization of cells in the cell population* [5, 10, 14, 24, 31]. Although the culture-doubling time is a macroscopic feature of the cell culture, it clearly depends on the properties of individual cells. The 'initial distribution of cells' refers to those cells present in the culture at time zero and the time when they first divide.

In the literature, we find the claim that the growth of various types of cells has certain qualitative features in common [35, p.1174]:

> "Studies during the past fifty years indicate that all cells grow in an essentially identical fashion, including those ranging from bacteria, yeasts, and protozoa to avian and mammalian cells."

and [11, p.1316] :

> "It is indeed striking that the growth characteristics found for Interleukin-2-dependent T-cells are identical to those of all other cells that have been examined, including bacteria, yeasts and protozoa, and all mammalian cells."

If one accepts these claims, then all mathematical models of cell growth should have certain features in common. However, certain terms in a mathematical model may have a significant quantitative effect in the study of cells of a given type, whilst being insignificant in the study of cells of a different type (or of similar cells under differing conditions).

In our view, some features of cell growth are typical of many other biological systems, such as population growth and immunological and epidemiological phenomena. Thus this paper may be of wider interest

than our title suggests. Quoting from [27],

> "… model selection is the most fundamental and crucial step in the study of all phenomena.".

However, there are also a number of factors that can give rise to different patterns of cell growth, for example, (i) the degree of synchronization of cells in the (initial) cell population, (ii) the homogeneity of the cell population, and (iii) the experimental conditions. Cells in an initially synchronized cell population are all assumed to be at the same point of the cell cycle at time zero, whereas cells in an homogeneous culture are all assumed to have the same growth characteristics, in particular, the same cell-division time.

1.2 Features of models

Both discrete and continuous models have been used to model cell growth. In the models that we consider, the time-lag τ actually corresponds to four distinguishable time-lags that represent: (i) the time between the start of the cell division process and the start of DNA synthesis (G_1 phase), (ii) the duration of the DNA synthesis (S phase), (iii) the time between the end of DNA synthesis and the start of mitosis (G_2 phase), and (iv) the duration of the mitosis stage (M phase), respectively. A simple discrete model for a synchronized and homogeneous (and hence synchronous [10, pp.153–168]) cell population is

$$N_{n+1} = 2N_n \quad \text{with } N_0 = N, \tag{1}$$

where $N_n = N(t_n)$, $t_{n+1} - t_n = \tau$ and $t_0 = 0$. The assumptions of this model are somewhat artificial, namely that *every* cell divides *exactly once* into *two viable* cells every τ hours *precisely*. Thus there is a jump in the size of the cell population every τ hours and a graph of $N(t)$, where $N(t)$ is a continuous extension of the discrete solution, resembles a staircase (see Fig. 1a). However, graphs of experimental data for synchronous cell growth typically only approximate a staircase due to, for example, variations in the cell-division time.

A common continuous model is the exponential growth model,

$$\frac{dN}{dt} = \rho_0 N(t) \quad \text{with } N(0) = N, \tag{2}$$

that has a strictly increasing solution for $\rho_0 > 0$ (see Fig. 1b). Between these two types of qualitative behaviour, there is a range of growth patterns, some of which are exhibited by the experimental data that we analyze.

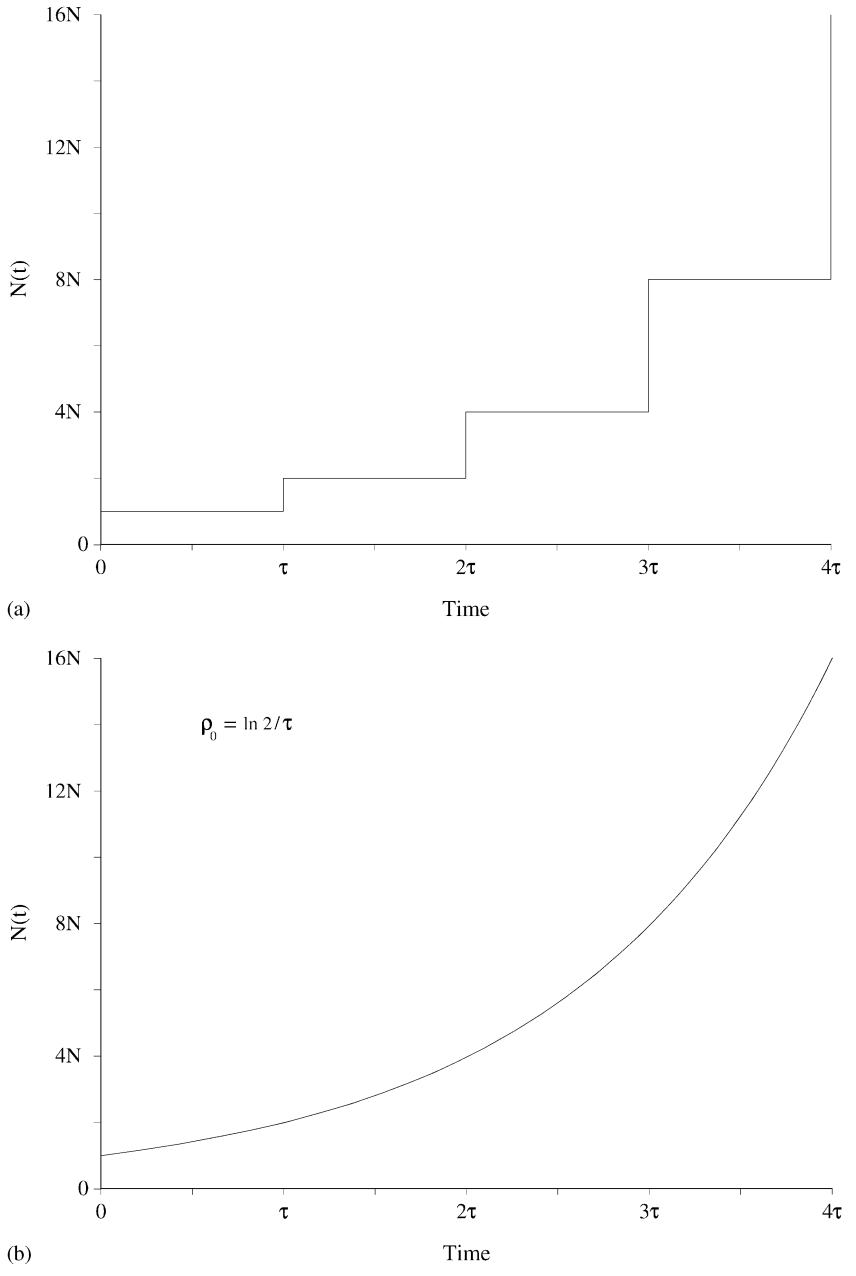

Fig. 1a, b. Graphs of idealized synchronous and exponential cell growth, respectively

For sufficiently large cell populations, continuous growth models can be used to approximate what is, essentially, a discrete process. Thus ordinary differential equations (ODEs) are frequently used to model cell growth. However, the discrete model (1) includes an explicit

time-lag τ that the simple ODE model (2) cannot model explicitly – some researchers have recognized that a time-lag (or delay) in the cell division phase suggests the use of delay differential equations (DDEs) rather than ODEs. Quoting from [23] :

> "A time delay between the beginning of activation" of cell division in T-cell dynamics "and the actual proliferation has therefore to be accounted for in the equations."

Indeed, some sets of experimental data clearly exhibit features that are consistent with there being a time-lag in the cell division phase [22, 24] (see Figs. 4 and 5a). In view of this, we compare how well two types of simple linear model (ones with a time-lag and ones without a time-lag) provide qualitative and quantitative consistency with some experimental cell growth data. More detailed models can be developed, see [9] and [26], for example.

1.3 Mathematical models

A good mathematical model should allow a phenomenon to be investigated by analyzing the features of the model. The model should be able to *predict new experimental observations* and to *determine the significance of each of the model parameters* (both *qualitatively* and *quantitatively*). Usually the simplest model that is *consistent with known data* is used, but a hierarchy of increasingly complex models can be developed with the aim of systematizing the process of model selection for specific types of data. Quoting from [27],

> "The highest level of sophistication of a model lies at the top of this hierarchy, a relatively unsophisticated model may rest at the lower end of the hierarchy. Which model is appropriate for a particular application is … determined through methods of *a posteriori* error estimation … ".

Thus, for example, a whole range of models have been used in the analysis of Interleukin-2-dependent T-cell growth, from models based on ODEs [20] to models based on DDEs [2, 36] and neutral delay differential equations (NDDEs) [23]. However, in some cases it is important to obtain accurate parameter values,[1] for example, in viral immunology where the T-cell proliferation parameters have a

[1] We require quantitative rather than qualitative consistency.

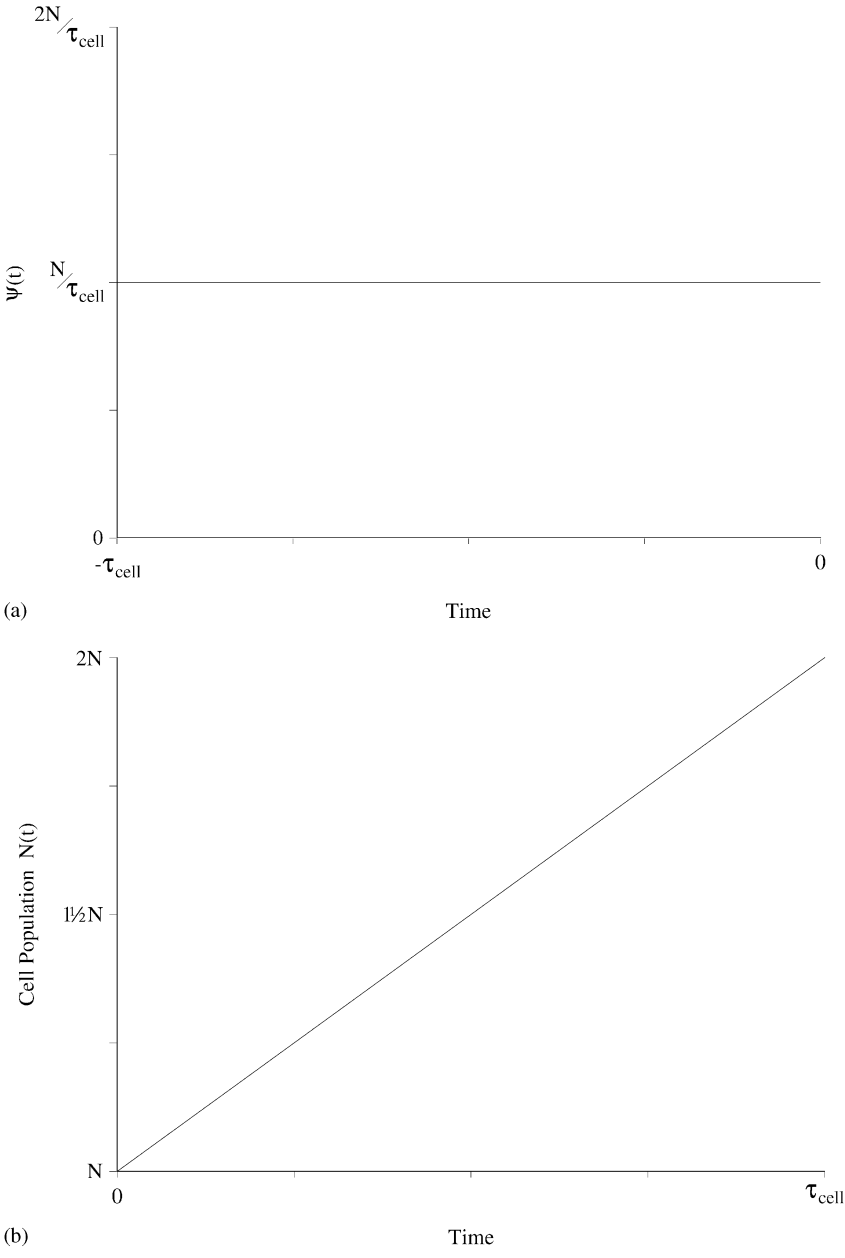

Fig. 2a–d. Graphs of $\psi(t)$ and $N(t)$ for the uniform and bell-shaped initial cell distributions

significant effect on the phenotype of the virus-host interaction [25]. Reliable parameter values can only be obtained if the right type of model is used. Another important question is whether any of the model parameters represent meaningful biological quantities.

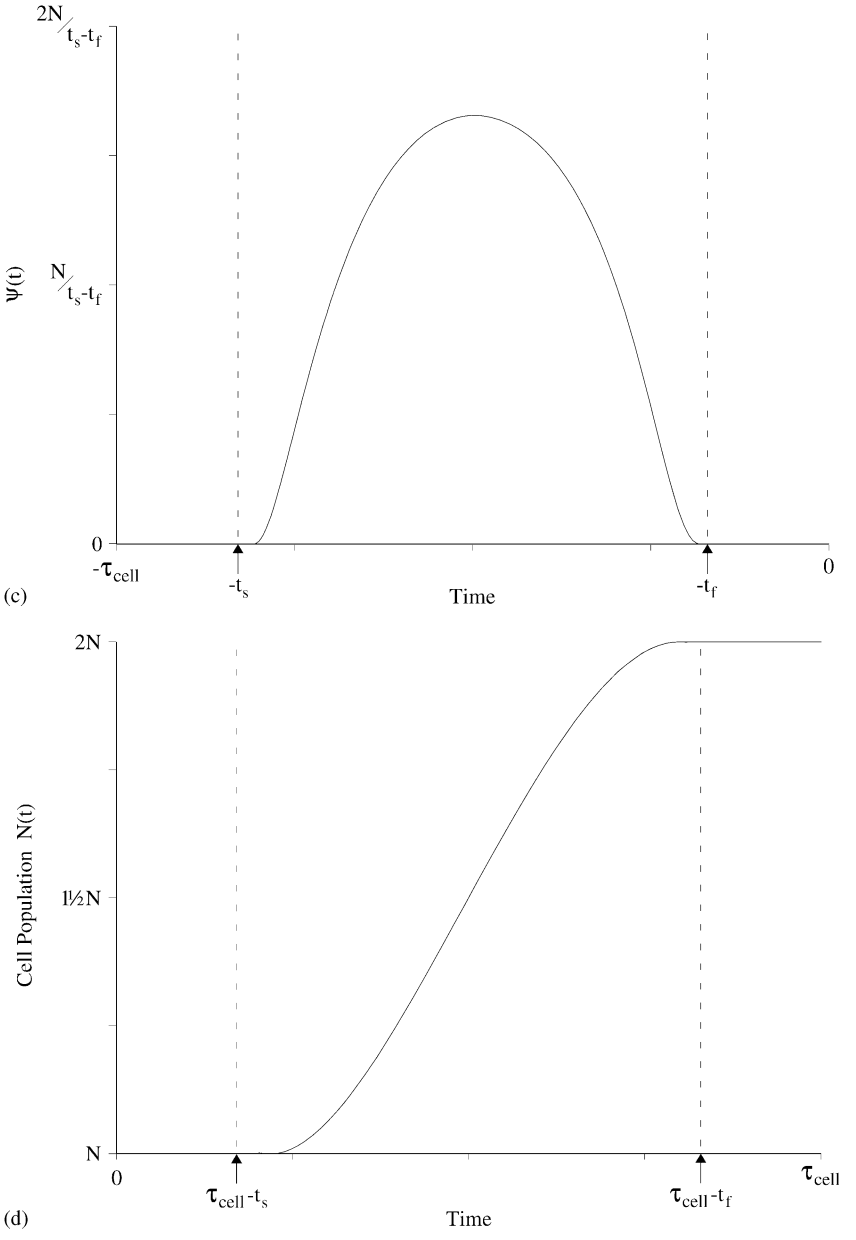

Fig. 2a–d. Continued

The precise mechanisms of cell growth are very complex, but both the *exponential growth model* (2) (an ODE model) and the general linear *time-lag growth model* (3) (an NDDE model) are quite simple. However, as we demonstrate in this paper, time-lag growth models can

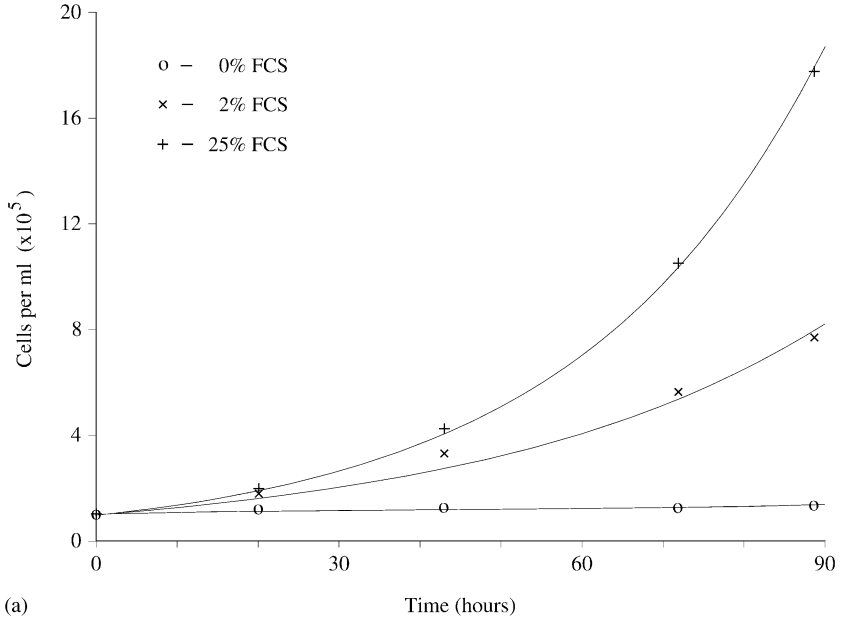

(a)

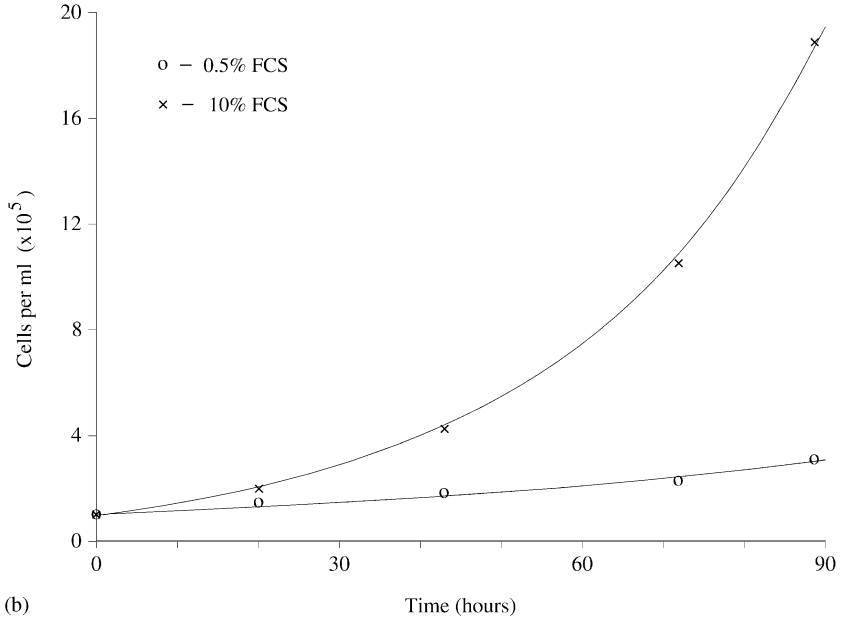

(b)

Fig. 3a and b. Pre-B-cells were grown at 37 °C in 5% CO_2 as single cell suspensions in RPMI 1640, supplemented with 10% FCS, 50U/ml penicillin, 50μg/ml streptomycin and 2mM L-glutamine. On day 0, cells were seeded out at a density of 1×10^5 cells/ml under the same conditions, except that the FCS concentration was varied. Continuous labelling with bromodeoxyuridine showed that the growth fraction was close to unity for all FCS concentrations down to 0.5%.

provide significant improvements in both the qualitative and quantitative consistency of the model with certain types of data. When developing a mathematical model, some researchers focus on the qualitative consistency of the model, and place less emphasis on the *quantitative consistency*. Indeed, some researchers avoid a particular mathematical model if no analytical closed-form solution exists. This can severely reduce the range of models throughout the model hierarchy and is, in fact, unnecessarily restrictive. For example, functional differential equation models would be restricted to linear problems, or non-linear problems of special types. The use of numerical methods, rather than analytical methods, to obtain a solution to the model equations greatly increases the range of available models. However, simple models can often provide genuine insight into the processes of cell division [15, 34].

Throughout this paper, we consider mathematical models based on three types of differential equation – ordinary, delay and neutral delay. Although analytical solutions exist for the ODE models, the same cannot be said for the DDE and NDDE models (except in special cases). The choice of differential equation used in our models takes into account the qualitative features of the experimental data. For example, Mitchison and Vincent [22] showed that the growth of several types of synchronous cell cultures has a common qualitative feature, namely prolonged (initial) step-like growth (cf. Fig. 1a). However, whilst it is impossible for the solution of an ODE to exhibit such behaviour, and extremely difficult to find a DDE that exhibits such behaviour (due to the smoothing of the solution), a simple NDDE can easily reproduce such behaviour (see Fig. 5b). Other types of differential equation model also appear in the literature, from Volterra functional differential equations [17, 33] to partial differential equations that have been used for modelling structured populations [9, 21, 32].

2 Some simple mathematical models

Our discussion should be of general interest because our mathematical models are not specific to the types of cell considered, but can be used in modelling many phenomena in which there is a time-lag. The models that we consider are selected from a hierarchy, the most complex model being

$$\begin{aligned} &\frac{dN}{dt} = \rho_0 N(t) + \rho_1 N(t - \tau_{\text{cell}}) + \rho_2 N'(t - \tau_{\text{cell}}) \quad (t \geqq 0)\,, \\ &N(t) = \Psi(t) \quad (-\tau_{\text{cell}} \leqq t < 0), \end{aligned} \tag{3}$$

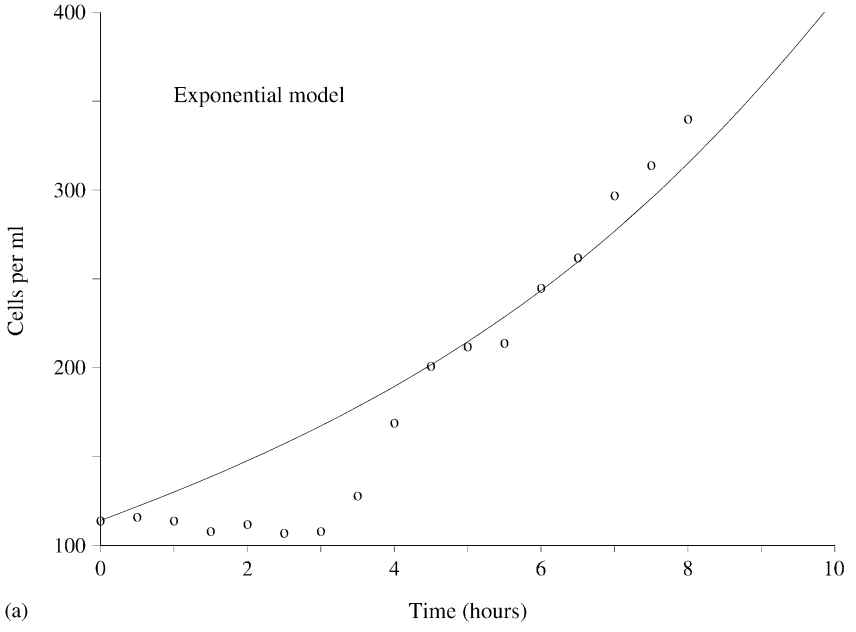

(a)

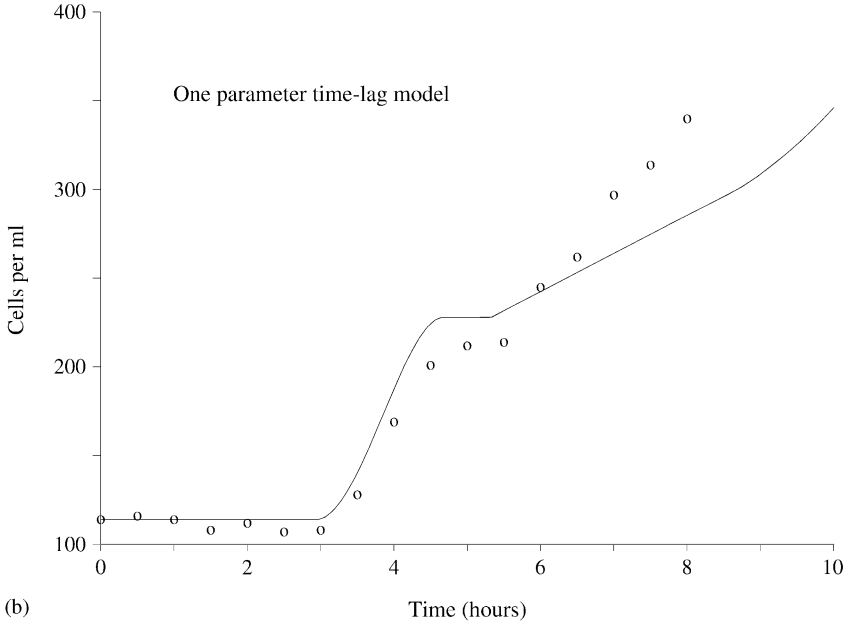

(b)

Fig. 4a–d. A culture of *cdc10-129 rum1Δ* fission yeast, *schizosaccharomyces pombe*, with deleted *rum*1-gene was grown in minimal medium at 25 °C and cells were synchronized using an elutriator rotor. The cells were then incubated at 36 °C, and samples taken every 30 minutes to measure the number of cells. The graphs

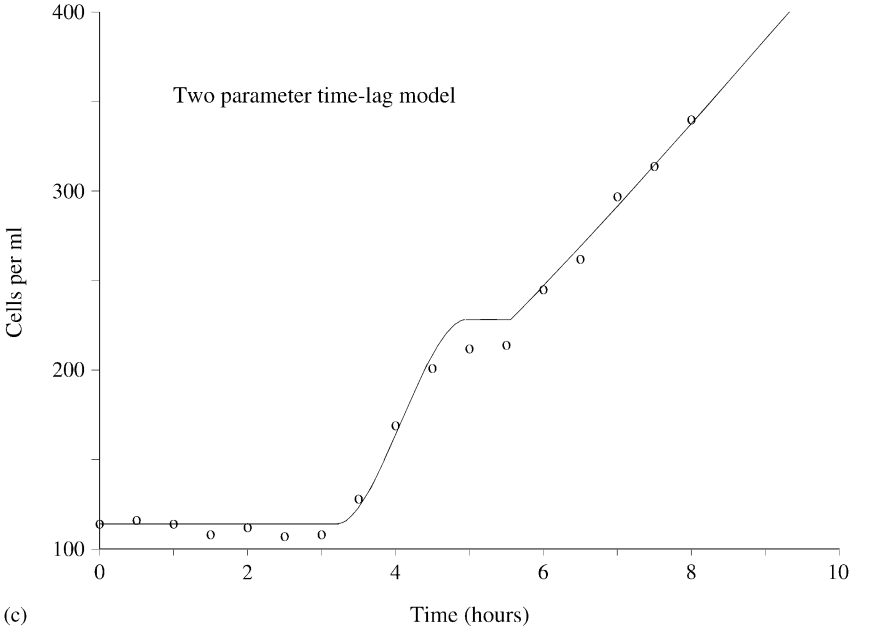

(c)

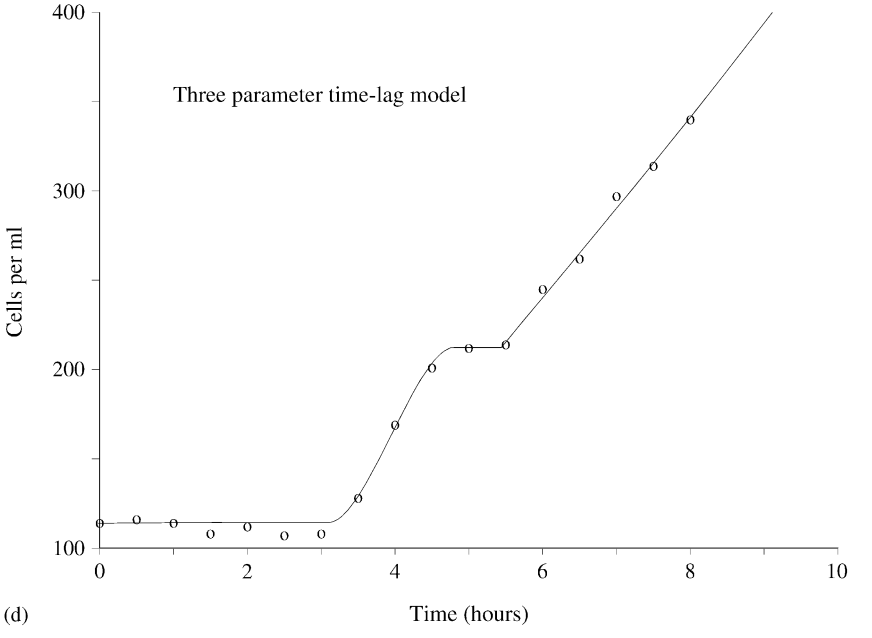

(d)

represent. **a** the exponential growth model, and the time-lag growth model fitting **b** τ_{cell}, **c** τ_{cell} and ρ_1, and **d** τ_{cell}, ρ_1 and β. The data given in Table 3a are represented by ○'s in the graphs.

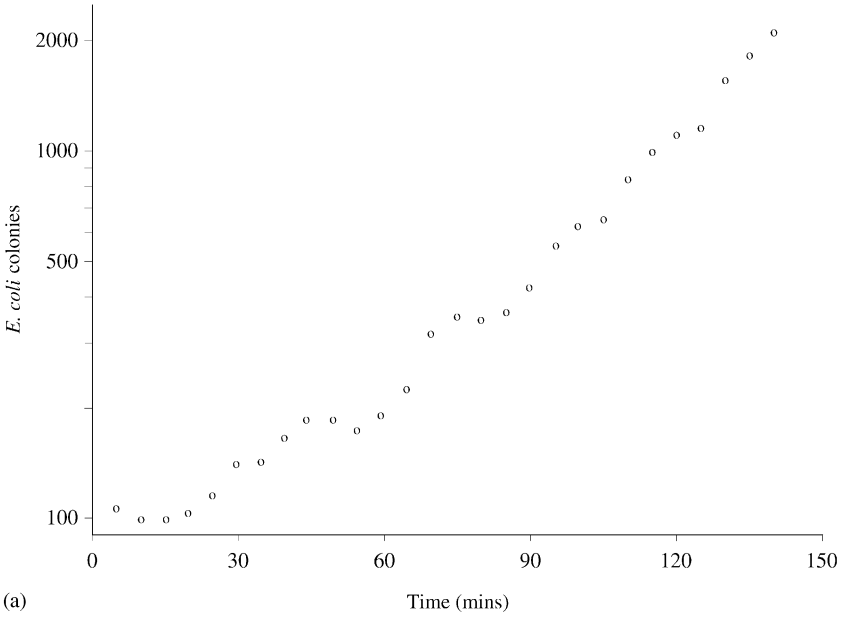

(a)

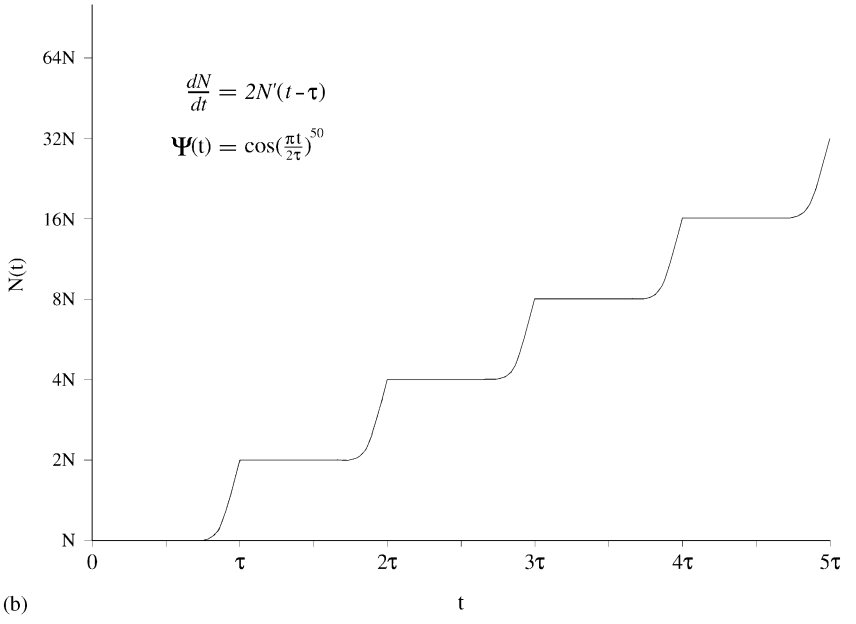

(b)

Fig. 5a and b. Data for synchronous *E. coli* growth and a graph of the solution of an NDDE.

Table 1. A biological interpretation of the parameters in the NDDE (3)

Parameter	Biological interpretation
$\tau_{\text{cell}} > 0$	The average cell-division time
$\rho_0 \geqq 0$	The proportionate rate of 'instantaneous' asynchronous cell growth
$\rho_1 \geqq 0$	The proportionate rate of 'delayed' asynchronous cell growth
$0 \leqq \rho_2 \leqq 2$	A measure of the proportionate rate of 'delayed' synchronous cell growth
$0 \leqq \beta \leqq 1$	The fraction of cells dividing over the first step

where $N'(t)$ is the right-hand derivative of $N(t)$ with respect to t and $N(0) = N$ is given. This equation is a linear NDDE with four scalar parameters ρ_0, ρ_1, ρ_2 and τ_{cell}. An additional parameter β may be introduced to model the fraction of cells that divide over the first step, so that $N(t) = \beta\Psi(t)$ for $t \in [-\tau_{\text{cell}}, 0)$. One possible biological interpretation of these parameters is given in Table 1.

By 'instantaneous' cell growth, we mean that the rate of growth is dependent on the *current* cell population and, similarly, by 'delayed' cell growth, we mean that the rate of growth is dependent on some *previous* cell population. In the case of idealized synchronous growth, $\rho_0 = 0$, $\rho_1 = 0$ and $\rho_2 = 2$, so that the degree of synchronization of cells in the cell population remains constant, but it should be noted that the effects of synchronizing a cell culture are usually only temporary. It should also be noted that the method of synchronizing the cells may damage the cell culture [13] and result in the initial cell growth being less than would otherwise be predicted.

The simplest model based on (3) is the *exponential growth model*,

$$\frac{dN}{dt} = \rho_0 N(t) \quad (t \geqq 0)\,, \tag{4}$$

with $N(t) = N\exp(\rho_0 t)$ for $t \geqq 0$. Another model based on (3) is the *time-lag growth model*

$$\begin{aligned} &\frac{dN}{dt} = \rho_1 N(t - \tau_{\text{cell}}) \quad (t \geqq 0), \\ &N(t) = \Psi(t) \quad (-\tau_{\text{cell}} \leqq t < 0). \end{aligned} \tag{5}$$

This DDE may be solved by repeated integration over intervals of length τ_{cell} or, using Laplace transform techniques, be expressed as an integral in the complex plane.

One of our aims is to demonstrate the *qualitative* and *quantitative* differences between different models based on (3). In general, the

existence of closed-form solutions of (4) and (5) is of little practical use when it comes to estimating parameter values, especially since closed-form solutions do not exist for most non-linear models. In practice, (approximate) solutions are obtained numerically (see Sect. 3.1), and so a much wider range of models can be considered.

2.1 The exponential growth model

The exponential growth model (4) has been used to model various types of cell growth [19, 31]. The rate of growth of the number of cells $N(t)$ is proportional to $N(t)$: that is to say, $dN/dt = \rho_0 N(t)$, where ρ_0 is the growth rate. Only the culture-doubling time, $\tau_{\text{culture}} = \ln(2)/\rho_0$, can be estimated from the exponential growth model. Further limitations of this model are discussed in [31], quoting from the abstract:

> When certain assumptions are not satisfied "the use of the exponential growth equation leads to errors in the determination of both population and cell generation time."

It has also been noted in [5, 16] that if the fraction of proliferating cells is less than unity, or cell growth is not exponential, then the relation of τ_{culture} to the (biologically meaningful) average cell-division time τ_{cell} is unclear.

2.2 A time-lag growth model

Some researchers have recognized that the use of DDEs greatly increases the range of qualitative behaviour that can be modelled accurately [8, 18]. The extension of the exponential growth model (4) by the inclusion of a delay can be justified by assuming that cells are initially inactive and that, once activated, cell division is not instantaneous. (Thus the culture-doubling time τ_{culture} is estimated by τ_{cell}.) The rate at which new cells appear at time $t \geqq \tau_{\text{cell}}$ is proportional to the number of cells at time $t - \tau_{\text{cell}}$, where τ_{cell} is the average cell-division time:[2] that is to say, $dN/dt = \rho_1 N(t - \tau_{\text{cell}})$, where ρ_1 is the growth rate. It is necessary to specify a function $\psi(t)$ over the initial interval $[-\tau_{\text{cell}}, 0)$ that defines the rate at which new cells appear over the interval $[0, \tau_{\text{cell}})$. Thus $N(t) = N + \int_0^t \psi(s - \tau_{\text{cell}})\, ds$ for $t \in [0, \tau_{\text{cell}})$. Assuming

[2] If τ_{cell} is "small", the data may be inadequate to distinguish between the two types of model.

that each cell divides at most once over the interval $[0, \tau_{\text{cell}})$, we have that $\int_0^{\tau_{\text{cell}}} \psi(s - \tau_{\text{cell}})\, ds \leqq N$. The function $\psi(t)$ represents the initial distribution of cells in the cell culture (cf. [10, Chap. 2]) and models the initial inhomogeneity in the cell population – including variations in the cell-division time of individual cells (that are normally distributed when examined as a function of the cell-division rate [1, 11]). The value of $\psi(t - \tau_{\text{cell}})$ gives the number of cells that are present in the culture at time zero that divide for the first time at time t. An assumption in our model is that no cell divisions occur before time zero, so that $N'(t) = 0$ for $t \in [-\tau_{\text{cell}}, 0)$. We introduce the initial function

$$\Psi(t) = \frac{1}{\rho_1}\psi(t)\,,$$

so that[3]

$$\frac{dN}{dt} = \rho_1 N(t - \tau_{\text{cell}}) \quad (t \geqq 0), \qquad N(t) = \Psi(t) \quad (-\tau_{\text{cell}} \leqq t < 0)\,.$$

We consider two initial functions that correspond to different initial distributions of cells over the cell cycle. In both cases, $\psi(t) \geqq 0$ and we assume that $\int_0^{\tau_{\text{cell}}} \psi(s - \tau_{\text{cell}})\, ds = N$:

Uniform distribution (*asynchronous growth*). Initially the cells are assumed to be uniformly distributed over the cell cycle, or the variation in the duration of the cell-cycle is comparable with the length of the cell cycle itself [11, 12, 14, 37]. In this case $\psi(t) = N/\tau_{\text{cell}}$, so that $dN/dt = N/\tau_{\text{cell}}$ for $t \in [0, \tau_{\text{cell}})$. Thus there is a steady appearance of cells over the interval $[0, \tau_{\text{cell}})$ (see Figs. 2a and b).

Bell-shaped distribution (*synchronized growth*). A bell-shaped initial function corresponds to non-monotone cell growth. The cells are assumed to be initially synchronized and have a low variability in their growth characteristics [11, 12, 24, 30]. The function $\psi(t)$ is defined in terms of the bell-shaped function $E(t)$ [7], where

$$E(t) = \begin{cases} \exp[-1/(1 - t^2)] & \text{for } |t| < 1, \\ 0 & \text{for } |t| \geqq 1. \end{cases} \tag{6}$$

$\psi(t)$ is taken as a multiple of $E((2t + (t_s + t_f))/(t_s - t_f))$, where $\tau_{\text{cell}} - t_s$ and $\tau_{\text{cell}} - t_f$ $(0 \leqq t_f < t_s \leqq \tau_{\text{cell}})$ specify when the first generation of cells starts and finishes appearing, respectively (*see* Figs. 2c and d).

[3] The experiment is assumed to start at time $t = 0$. However it would not be correct to interpret $\Psi(t)$ as the number of cells $N(t)$ for $t \in [-\tau_{\text{cell}}, 0)$, rather that $\rho_1 \Psi(t - \tau_{\text{cell}})$ corresponds to the rate of cell growth dN/dt for $t \in [0, \tau_{\text{cell}})$.

3 Numerical methods

There is a substantial literature on the numerical solution of DDEs [4]. The numerical methods used for solving the parameter estimation problems in this paper are discussed in [28]. Some of the difficulties that can arise when estimating parameters in NDDEs, and references to other work in this area, appear in [3].

3.1 NDDE solvers

Codes for solving NDDEs numerically are based on ODE solvers. However, when adapting an ODE solver, there are several issues that must be addressed [4]:

- The provision of a suitable – robust, but reasonably cheap – continuous extension (dense output) for evaluating delayed solution and derivative terms.
- The effect and propagation of jump discontinuities in derivatives of the solution.
- The treatment of 'small' delays when using explicit solution methods.

There are a number of codes available for solving evolutionary DDEs. A feature of such codes is that they (aim to) produce a numerical solution to within a requested accuracy. Paul [28] has written such a code based on the Dormand and Prince fifth-order Runge–Kutta ODE method and a fifth-order Hermite interpolant due to Shampine. The code is uniformly fifth-order accurate for ODEs, DDEs and NDDEs.[4]

3.2 Parameter estimation for NDDEs

The task of parameter estimation is one of minimizing an objective function $\Phi(\mathsf{p})$, say, based on unknown parameters p and sample data $\{z_i, N(z_i)\}$. In the case of NDDEs, this can mean estimating the initial values and parameters in the derivatives (as in the ODE case), but also estimating the position of the initial point, (parameters in) the initial functions, (parameters in) the initial derivatives and (parameters in) the delay functions.

[4] The code is available for non-commercial use by emailing na.cpaul@na-net.ornl.gov.

Consider, for example, estimating (some of) the parameters in the NDDE (3): Given an initial value N and initial function $\Psi(t)$ for $t \in [-\tau_{\text{cell}}, 0)$, each set of parameter values defines a solution $N(t) \equiv N(t; \mathsf{p})$, where $\mathsf{p} = [\rho_0, \rho_1, \rho_2, \tau_{\text{cell}}, \beta]$. The *optimum* least-squares parameters p^* satisfy $\Phi(\mathsf{p}^*) \leqq \Phi(\mathsf{p})$ for all admissible values of p and p^*, where

$$\Phi(\mathsf{p}) := \sum_{i=1}^{n} (N(z_i; \mathsf{p}) - N(z_i))^2. \tag{7}$$

There are two types of numerical method for finding p^*, derivative-free methods and those that use derivatives of $\Phi(\mathsf{p})$. However, in general, the solution of a (neutral) DDE has jump discontinuities in its derivatives, in the case of (3) at points $k\tau_{\text{cell}}$ for $k = 1, 2, \ldots$. These discontinuities can propagate into the objective function, so that $\Phi(\mathsf{p})$ and its derivatives suffer jumps. In the case of (3), for example, a jump in $N'(t; \mathsf{p})$ propagates into $\Phi(\mathsf{p})$ when the time-lag τ_{cell} is being estimated and the position of the jump in $N'(t; \mathsf{p})$ crosses a data point z_i as τ_{cell} varies. A detailed discussion of the mechanism by which jump discontinuities propagate into $\Phi(\mathsf{p})$ appears in [3].

A method of finding the optimum parameter values is as follows: First, the model equations are solved using the current (initial) parameter values p and then the value of the objective function $\Phi(\mathsf{p})$ is calculated. Next, the minimization algorithm adjusts the parameter values so as to reduce the value of $\Phi(\mathsf{p})$. Finally, when no further reduction in the value of $\Phi(\mathsf{p})$ is possible, the (*local*) best-fit parameter values have been found. In order to find the *global* best-fit (and hence optimum) parameter values p^*, the initial parameter values must be sufficiently close to p^*. Thus good initial parameter estimates are essential if p^* is to be found. Such estimates can sometimes be found by modelling a sequence of subsets of the experimental data; as the size of the subset increases, the estimate of the best-fit parameter values improves. This approach can be very efficient when solving some immune response models [7, 18].

There are several least-squares minimization codes available,[5] for example, E04UPF in the NAG library, LMDIF from NETLIB and fmins in MATLAB. However, a number of points should be noted:

- Usually the model solution values $\{N(z_i, \mathsf{p})\}$ are obtained numerically.
- The effect of the limited accuracy of $\{N(z_i, \mathsf{p})\}$ on the minimization code should be assessed, especially when finite-difference methods are used to approximate derivatives of $\Phi(\mathsf{p})$.

[5]In this paper, we used LMDIF that solves *unconstrained* least-squares minimization problems.

- It is generally assumed that $\Phi(\mathbf{p})$ is sufficiently smooth *everywhere* but, when estimating parameters in DDEs and NDDEs, $\Phi(\mathbf{p})$ can be discontinuous almost *anywhere* [3].
- The chances of finding $\mathbf{p}^*$ can be improved by specifying lower and/or upper bounds on the parameter values (using *a priori* information).
- The computational effects of variations in scale between parameter values can be reduced by rescaling the parameters to be of the same order of magnitude.

3.3 Sensitivity analysis

One of the aims of the mathematical modelling of cell growth is to provide reliable estimates of biological parameters. Thus, having determined a best-fit set of parameter values, it is useful to have some indication of the standard deviation of each parameter value. However, one of the underlying statistical assumptions that allows the standard deviations to be estimated is that the parameter estimation problem is (almost) linear. One method of assessing the impact of non-linearity is to determine the bias of each parameter value due to the non-linearity of the problem [29, Sect. 2.6]. If this non-linear bias is small, usually less than 1%, then the parameter estimates and their standard deviations can be considered to be reliable.

One approach for estimating the standard deviations $\{\sigma(\mathbf{p}_i)\}_{i=1}^{r}$ of the parameter values $\mathbf{p}$ is given in [6, pp. 206–208]. The method uses the Hessian $H(\mathbf{p})$ of the objective function to approximate the covariance matrix $[\varsigma_{ij}]$, where

$$[\varsigma_{ij}]_{i,j=1}^{r} = 2\frac{\Phi(\mathbf{p})}{n-r}H^{-1}(\mathbf{p})$$

and $n-r$ is the number of degrees of freedom. However, in our case, the Hessian $H(\mathbf{p})$ must itself be estimated using

$$H(\mathbf{p}) = \left[\frac{\partial^2\Phi}{\partial\mathbf{p}_i\partial\mathbf{p}_j}\right]_{i,j=1}^{r} \approx 2\left[\sum_{k=1}^{n}\frac{\partial N(z_k;\mathbf{p})}{\partial\mathbf{p}_i}\frac{\partial N(z_k;\mathbf{p})}{\partial\mathbf{p}_j}\right]_{i,j=1}^{r}.$$

An estimate of the standard deviation of the parameter $\mathbf{p}_i$ is then given by $\sigma(\mathbf{p}_i) = \sqrt{\varsigma_{ii}}$.

The sensitivity coefficients $\{\partial N(z_k;\mathbf{p})/\partial\mathbf{p}_i\}$ are obtained by differentiating equation (3) with respect to the parameter $\mathbf{p}_i$, integrating the resulting differential equation with respect to t, and evaluating the solution at the data points z_k for $k = 1, 2, \ldots, n$. For

example,

$$N'_{\rho_0}(t;\mathbf{p}) = N(t;\mathbf{p}) + \rho_0 N_{\rho_0}(t;\mathbf{p}) + \rho_1 N_{\rho_0}(t-\tau_{\text{cell}};\mathbf{p}) + \rho_2 N'_{\rho_0}(t-\tau_{\text{cell}};\mathbf{p})$$
$$(t \geqq 0),$$

where

$$N_{\rho_0}(t;\mathbf{p}) \equiv \frac{\partial N}{\partial \rho_0} \text{ with } N_{\rho_0}(t;\mathbf{p}) = \frac{\partial \Psi}{\partial \rho_0} \text{ for } t \in [-\tau_{\text{cell}}, 0) .$$

Similar equations can be obtained for $N'_{\rho_1}(t;\mathbf{p})$, $N'_{\rho_2}(t;\mathbf{p})$ and $N'_{\beta}(t;\mathbf{p})$, but $N'_{\tau_{\text{cell}}}(t;\mathbf{p})$ satisfies

$$N'_{\tau_{\text{cell}}}(t;\mathbf{p}) = \rho_0 N_{\tau_{\text{cell}}}(t;\mathbf{p}) + \rho_1 N_{\tau_{\text{cell}}}(t-\tau_{\text{cell}};\mathbf{p}) - \rho_1 N(t-\tau_{\text{cell}};\mathbf{p})$$
$$+ \rho_2 N'_{\tau_{\text{cell}}}(t-\tau_{\text{cell}};\mathbf{p}) - \rho_2 N''(t-\tau_{\text{cell}};\mathbf{p}) , \quad (t \geqq 0) \tag{8}$$

where

$$N'_{\tau_{\text{cell}}}(t;\mathbf{p}) = \frac{d}{dt}\frac{\partial N}{\partial \tau_{\text{cell}}} \text{ with } N_{\tau_{\text{cell}}}(t;\mathbf{p}) = \frac{\partial \Psi}{\partial \tau_{\text{cell}}} \text{ for } t \in [-\tau_{\text{cell}}, 0) .$$

Equation (8) may be solved directly, given a suitable approximation to $N''(t;\mathbf{p})$ [38, p. 121], or may be rewritten as a pair of first-order NDDEs provided that $N'(t)$ and $N''(t)$ are always taken as being right-hand derivatives and the jump discontinuities in $N(t)$ and its derivatives are treated appropriately.

4 Patterns of cell growth

We analyze three different patterns of cell growth in order to demonstrate the qualitative and quantitative differences between various models in our hierarchy. The qualitative fit is indicated by a graph of the best-fit solution and the experimental data, whilst the quantitative fit is indicated by the norm of the residual vector $\|\text{Err}\|_2 = \sqrt{\Phi(\mathbf{p}^*)}$ and the standard deviations of the best-fit parameter values. The reliability of the parameter values is also dependent on the non-linearity of the parameter estimation problem, and so each parameter value is given with an estimate of its non-linear bias in the form 'parameter (bias%)'.

The first set of data exhibits 'classic' exponential growth, the second set exhibits initial step-like growth that rapidly smooths, and the final set exhibits prolonged step-like growth.

4.1 Pre-B-cell growth in fetal calf serum

We consider experimental data for the growth of *Reh* cells of haematopoietic origin (pre-B-cells) in different concentrations of fetal calf serum (FCS) [16]. In obtaining data from the graphs in [16], we took the average value of the range of values for the cell concentration. Features of the model are: (i) The initial cell population is uniformly distributed between the $(G_0 + G_1)$-phases and the $(S + G_2 + M)$-phases of the cell cycle. (ii) The growth fraction is close to unity. When specifying a time-lag model, (i) implies that $\Psi(t) = N$ and (ii) implies that $\rho_1 = 1/\tau_{\text{cell}}$. The optimum parameter values for modelling the data in Table 2a appear in Table 2b.

Table 2a. Data for pre-B-cell growth at different concentrations of fetal calf serum

	Data				
Time (hrs)	0.0	20.0	42.9	71.8	88.6
Data set	Concentration (cells/ml)				
0% FCS	1.0×10^5	1.20×10^5	1.26×10^5	1.25×10^5	1.34×10^5
0.5% FCS	1.0×10^5	1.47×10^5	1.83×10^5	2.29×10^5	3.10×10^5
2% FCS	1.0×10^5	1.97×10^5	3.29×10^5	5.62×10^5	7.68×10^5
10% FCS	1.0×10^5	2.07×10^5	4.23×10^5	10.50×10^5	17.75×10^5
25% FCS	1.0×10^5	2.07×10^5	4.23×10^5	10.50×10^5	18.86×10^5

Table 2b. Least-square estimates and standard deviations of the parameters for pre-B-cell growth

	Exponential model			Time-lag model		
Data set	τ_{culture} (hrs)	$\sigma(\tau_{\text{culture}})$	$\|\|\text{Err}\|\|_2$	τ_{cell} (hrs)	$\sigma(\tau_{\text{cell}})$	$\|\|\text{Err}\|\|_2$
0% FCS	194.9 (3.31%)	28.1	0.166×10^5	241.1 (3.34%)	36.1	0.153×10^5
0.5% FCS	55.27 (0.38%)	1.89	0.285×10^5	51.38 (0.30%)	1.63	0.233×10^5
2% FCS	29.65 (0.19%)	0.60	0.769×10^5	25.84 (0.19%)	0.38	0.525×10^5
10% FCS	21.31 (0.01%)	0.06	0.313×10^5	18.22 (0.00%)	0.01	0.062×10^5
25% FCS	20.95 (0.01%)	0.06	0.322×10^5	17.90 (0.02%)	0.08	0.523×10^5

The values of τ_{culture} and τ_{cell} in Table 2b indicate that increasing the concentration of FCS reduces the cell-division time. The quantitative consistency of the exponential growth model (4) and time-lag growth model (5) with the data is indicated by the size of $||\text{Err}||_2$. The non-linear bias in the parameter estimates for the 0% FCS data is explained by the fact that one of the assumptions of our mathematical model, namely that the growth fraction is close to unity, is not satisfied. The qualitative consistency of the models is indicated by the graphs in Fig. 3, where the graphs for the exponential model and time-lag model are identical.

Although the estimates of τ_{culture} are consistently higher than the estimates of τ_{cell} (except when the FCS concentration is 0%), the standard deviations of the parameter values are similar. However, the exponential model cannot provide estimates of the average cell-division time, the rate of commitment of cells to cell division, or the initial distribution of cells in the cell cycle.

4.2 Growth of fission yeast

We analyze the growth of *fission yeast* using data that does not exhibit exponential growth [24]. (Non-exponential growth has also been reported for other types of cells [5, 31].) The data for yeast growth are given in Table 3a (see [24, Fig. 4f]). Features of the model are: (i) The cell growth is not exponential. (ii) The cells are synchronized at time zero. When specifying a time-lag model, (ii) implies that the bell-shaped initial function (6) should be used rather than a constant initial function.

Once again, the exponential growth model can only provide an estimate of the culture-doubling time τ_{culture}. However, depending on the number of parameters being estimated, the time-lag growth model (5) can provide estimates of the average cell-division time τ_{cell}, the fraction β of cells dividing over the first step, and the rate of commitment of cells ρ_1 to cell division (see Table 3b). Using the values $t_s = 2.5$ hrs. and $t_f = 0.5$ hrs. in the bell-shaped function (see [24] for the septation index), we obtain:

- Fit τ_{cell} with $\beta = 1$, $\rho_1 = 1/\tau_{\text{cell}}$ and $\Psi(t) = \gamma N \tau_{\text{cell}} E(t + 1.5)$ (see Fig. 4b).
- Fit τ_{cell} and ρ_1 with $\beta = 1$ and $\Psi(t) = \gamma(N/\rho_1)E(t + 1.5)$ (see Fig. 4c).
- Fit τ_{cell}, ρ_1 and β with $\Psi(t) = \gamma(N\beta/\rho_1)E(t + 1.5)$ (see Fig. 4d).

(The scaling factor $\gamma \approx 2.25$ ensures that $\int_0^{\tau_{\text{cell}}} \psi(s - \tau_{\text{cell}})\, ds = N$.)

The quantitative consistency of the exponential model is worse than that of the time-lag model (as measured by $||\,\text{Err}\,||_2$). Table 3b also

Table 3a. Data for non-exponential fission yeast growth

Data																
Time (hrs)	0.0	0.5	1.0	1.5	2.0	2.5	3.0	3.5	4.0	4.5	5.0	5.5	6.0	6.5	7.0	7.5	8.0
Cells/ml	114	116	114	108	112	107	108	128	169	201	212	214	245	262	297	314	340

Table 3b. Least-squares estimates and standard deviations of the parameters for fission yeast growth

Exponential model			Time-lag model						
$\tau_{culture}$ (hrs)	$\sigma(\tau_{culture})$	$\|\|Err\|\|_2$	τ_{cell} (hrs)	$\sigma(\tau_{cell})$	ρ_1 (hr^{-1})	$\sigma(\rho_1)$	β	$\sigma(\beta)$	$\|\|Err\|\|_2$
5.44 (0.55%)	0.241	113	5.33 (0.15%)	0.163	–	–	–	–	86
–	–	–	5.58 (0.04%)	0.054	0.399 (0.34%)	0.018	–	–	28
–	–	–	5.45 (0.03%)	0.038	0.443 (0.06%)	0.014	0.864 (0.09%)	0.019	15

indicates that, as the number of parameters being estimated in the time-lag model increases, the quantitative consistency of the model with the data improves significantly. However, the standard deviations in Table 3b also indicate that, as the number of parameters being estimated in the time-lag model increases, the accuracy of the parameter estimates improves. We also note that the values of τ_{culture} and τ_{cell} for the three-parameter time-lag model are the same, although their standard deviations differ by a factor of 6. The qualitative consistency of the models is indicated by the graphs in Fig. 4.

4.3 Growth of Escherichia coli colonies

We model a synchronous culture of *E. coli* colonies that exhibits prolonged step-like growth [22, Fig. 4]. The term 'synchronous' refers to the fact that the cells in the culture are homogeneous and synchronized [10]. Thus features of the model are: (i) All the cells have the same division time. (ii) All the cells divide simultaneously. (iii) There is prolonged initial step-like growth. (iv) The initial number of *E. coli* colonies is unknown. When specifying a time-lag model, (ii) implies that the bell-shaped initial function (6) should be used, and (iii) suggests that a neutral delay term should be included in the time-lag model (for qualitative reasons). The values of t_s and t_f required for (6) do not appear in [22] so we have used $t_s = \tau_{\text{cell}}$ and $t_f = 0$, but they could equally be treated as parameters to be estimated. Also, because no cell divisions (are assumed to) occur before time zero, the initial derivative for (3) is $N'(t) = 0$ for $t \in [-\tau_{\text{cell}}, 0)$.

A significant qualitative feature of the data is the prolonged step-like growth pattern (see Fig. 5a). This pattern is typical of synchronous cell growth (cf. Fig. 1a) and is most easily modelled using a neutral delay term (see Fig. 5b). In Fig. 5b, steps occur in the solution of the NDDE at every multiple of τ, suggesting that an initial estimate of 20 minutes for τ_{cell} may be used for modelling the *E. coli*.

Another significant feature of the data is the fact that the initial (integer) number of *E. coli* colonies, N, is unknown. There are two solutions to this problem: (i) N can be specified as a parameter to be estimated, or (ii) N can be estimated by backwards continuation of the data. Two possible values for N are 114 (based on linear extrapolation from the first two data points) and 99 (treating the first data point as being spurious).[6]

[6] We use the value that provides the best-fit to the data.

The time-lag models that we consider are:

- Fit τ_{cell} with $\rho_0 = 0$, $\rho_1 = 1/\tau_{\text{cell}}$, $\rho_2 = 0$, $\beta = 1$ and $\Psi(t) = 2/\tau_{\text{cell}} \times \gamma N \tau_{\text{cell}} E(2t/\tau_{\text{cell}} + 1)$ (see Fig. 6b).
- Fit τ_{cell}, ρ_0 and ρ_1 with $\rho_2 = 0$, $\beta = 1$ and $\Psi(t) = 2/\tau_{\text{cell}} \times \gamma(N/\rho_1) E(2t/\tau_{\text{cell}} + 1)$ (see Fig. 6c).
- Fit τ_{cell}, ρ_0, ρ_1, ρ_2 and β with $\Psi(t) = 2/\tau_{\text{cell}} \times \gamma(N\beta/\rho_1) E(2t/\tau_{\text{cell}} + 1)$ (see Fig. 6d).

It is clear from Table 4b and the graphs in Fig. 6 that the hierarchy of NDDE models provides better qualitative and quantitative consistency with the data than the exponential model. In the five parameter time-lag model, the value of β indicates that only a small fraction of the *E. coli* colonies divide over the first interval $[0, \tau_{\text{cell}}]$. This observation is confirmed by analyzing the data in Table 4a where, despite an initial reduction in the number of *E. coli* colonies, during the first 25 minutes there is only a 15% increase in the number of *E. coli* colonies. However, as Mitchison and Vincent [22] remark,

> "There may also be a lag before the synchronous culture attains its full growth rate … ",

and so this behaviour is not unexpected. Also, the values $\rho_0 \approx 0$, $\rho_1 \approx 0$ and $\rho_2 = 1.87$ indicate that the *E. coli* colonies slowly become desynchronized over time (*see below*), and this can be seen in the graph of the data (Fig. 5a). Our biological interpretation of equation (3) is that the ODE term corresponds to the *instantaneous* death of *E. coli* colonies, and the delay and neutral delay terms correspond to the asynchronous and synchronous growth of *E. coli* colonies, respectively.

Synchronous cultures have been analyzed by Engelberg and Hirsch [10, pp. 14–37]: They note that the degree of synchronization of cells in a synchronous culture decreases with time, so that the culture approaches 'steady exponential growth'. They also comment that

> "… the growth curve needs to be analyzed during the period of the decay of synchronization of cell division; the greater the degree of (initial) synchronization of the culture, the greater the accuracy with which the doubling-time distribution can be calculated from the growth data."

5 Further work

Mathematical modelling is more of an art than a precise science. Whilst the initial choice of mathematical model may be strongly

Table 4a. Data for the growth of a synchronous culture of *E. coli* colonies

Data														
Time (mins)	4.85	9.96	15.1	19.6	24.6	29.5	34.6	39.4	43.9	49.4	54.3	59.2	64.5	69.5
Colonies	106	99	99	103	115	140	142	165	185	185	173	190	224	317
Time (mins)	74.9	79.8	85.0	89.7	95.2	99.7	105	110	115	120	125	130	135	140
Colonies	353	346	363	424	551	623	650	836	992	1105	1153	1556	1818	2100

Table 4b. Initial values, least-squares estimates and standard deviations of the parameters for *E. coli* growth

Exponential model											
N	τ (mins)	$\sigma(\tau)$									$\|\|Err\|\|_2$
99	33.6 (0.06%)	0.457									725

Time-lag model											
N	τ (mins)	$\sigma(\tau)$	ρ_0 (min^{-1})	$\sigma(\rho_0)$	ρ_1 (min^{-1})	$\sigma(\rho_1)$	ρ_2	$\sigma(\rho_2)$	β	$\sigma(\beta)$	$\|\|Err\|\|_2$
99	28.8 (0.11%)	0.601	–	–	–	–	–	–	–	–	807
114	27.6 (0.13%)	0.570	-1.12×10^{-1} (0.62%)	0.008	3.03×10^{-1} (0.87%)	0.021	–	–	–	–	259
114	20.2 (0.03%)	0.086	-3.56×10^{-3} (0.05%)	0.004	8.63×10^{-3} (0.04%)	0.008	1.87 (0.06%)	0.067	0.158 (0.03%)	0.040	127

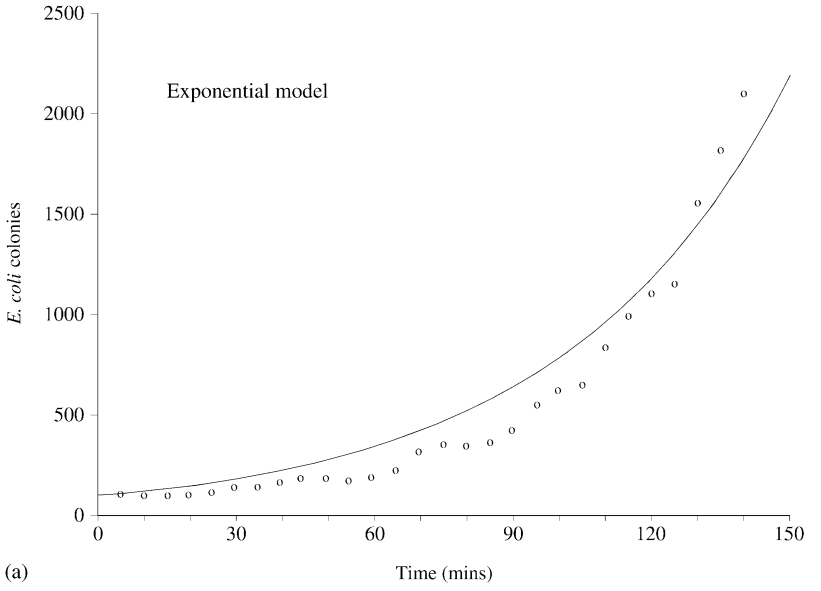

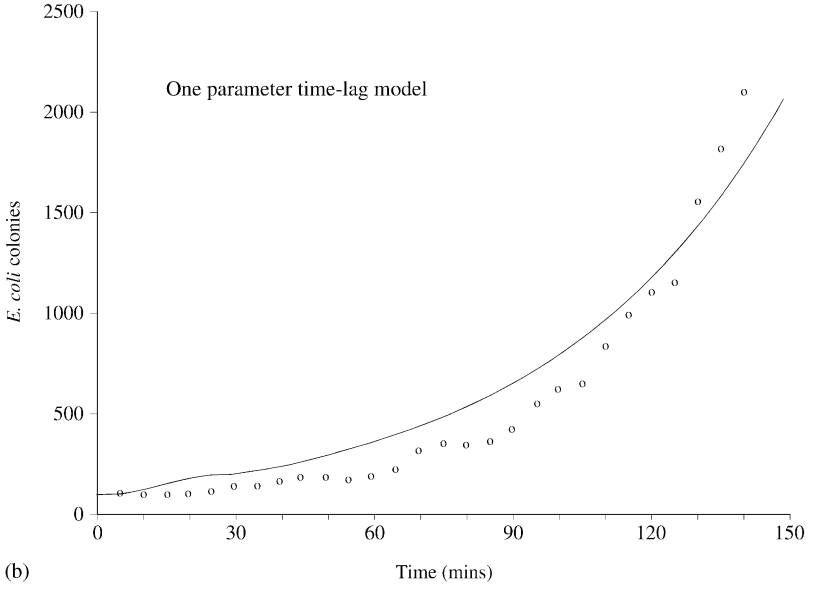

Fig. 6a–d. A synchronous culture of *E. coli* K12λ F^- cells was prepared by loading 2×10^{10} cells from an exponential culture into a 15 ml tube. The cells were then centrifuged at 2500 g for 20 minutes and the top 2% of cells suspended in fresh growth medium. The graphs represent. **a** the exponential growth model, and the time-lag growth model fitting **b** τ_{cell}, **c** τ_{cell}, ρ_0 and ρ_1, and **d** τ_{cell}, ρ_0, ρ_1, ρ_2 and β.

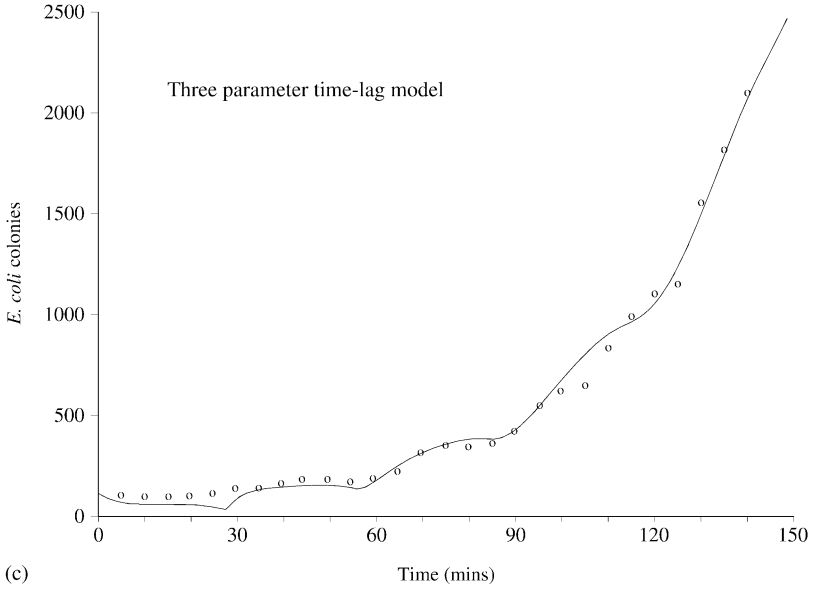

(c)

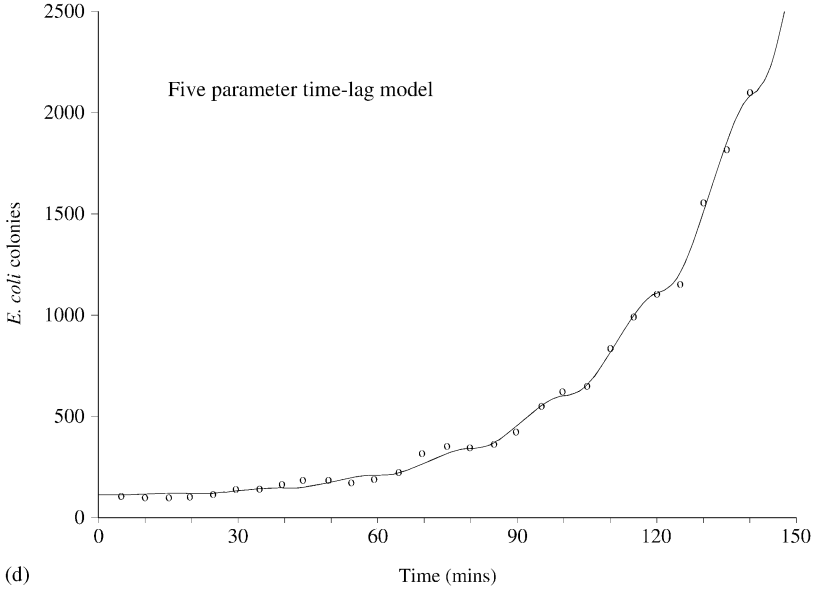

(d)

Fig. 6a–d. Continued

influenced by the pattern of cell growth, the precise development of the model hierarchy depends on intuition and deductions based on the nature of the experimental data and the biological processes being modelled. Whilst the models in this paper are, in some respects, quite simple because they only have a single, constant time-lag, more

complicated models can be developed that include separate time-lags for each stage of the cell-division process, or that have state-dependent time-lags that model environmental conditions such as the temperature, the level of nutrients, etc.

For a highly synchronized synchronous culture, an alternative to the bell-shaped initial function might be used, for example, one chosen solely for its qualitative properties (see Fig. 5b). In fact, it is possible to develop a hierarchy of initial functions that is independent of the model hierarchy. For example, for the *E. coli* growth, the observation that only a small proportion of *E. coli* colonies divide during the first interval suggests that the inclusion of the parameter β in the model is of some importance. (However, such an observation should not be unexpected because, as we have already noted, the synchronization process generally damages the cell culture so that the initial cell growth is usually less than predicted.)

Whilst we have used the least-squares objective function for determining the best-fit parameter values, there are many alternative objective functions: The *weighted* least-squares objective function can be used to take account of the relative significance of each datum, with small weights being assigned to data with (suspected) large errors and vice-versa. Alternatively, if there is considerable variation in scale between the experimental data, an objective function based on the relative error in fitting the data might be used. If the experimental data has significant qualitative features, then an objective function that also takes account of the rate of change of the data might be considered, in an attempt to preserve the 'shape' of the discrete data.

6 Conclusion

The work reported here provides scope for further analysis of suitable experimental data.

Sometimes a good qualitative but relatively poor quantitative model may be preferred to a good quantitative but relatively poor qualitative model. However, for idealized experimental data,[7] a good qualitative and quantitative model should exist. The determination of such a model is extremely difficult, if not impossible, but simple models can be progressively improved to take account of various qualitative

[7] In an ideal situation, there would be no variation in the conditions of the experiment and *all* aspects of the experiment could be measured precisely (without affecting the experiment).

features of the data and a better understanding of the processes being modelled. However, in order for (quantitative) mathematical modelling to be successful, it is necessary to have access to suitable *raw* experimental data. For example, data relating to the transient phases of the model is typically required for estimating kinetic parameters.

The increased complexity of the time-lag growth models seems to be justified, with the model parameters corresponding to experimentally measurable and controllable growth characteristics, and the models consistently providing better qualitative and quantitative fits to the data. However, it should be noted that the exponential growth model and the time-lag growth models form part of the same hierarchy of related models. In this hierarchy, estimates of parameters obtained from simpler models can be used as initial parameter estimates in more complex models. Thus the estimate of τ_{culture} from the exponential growth model can be used as an initial estimate for τ_{cell} in the time-lag growth models.

Acknowledgements. The authors express their thanks to Professor A.A. Romanyukha for valuable comments and to Drs. P. Foster and E. Kyprianou for checking various aspects of the manuscript. Support from the EPSRC Mathematics Programme, the Manchester University Research Support Fund, the fSU programme of the London Mathematical Society, and the Russian Foundation for Basic Research is gratefully acknowledged.

References

1. Bailey, J. E., Ollis, D. F.: Biochemical engineering fundamentals (2nd edition) New York: McGraw Hill 1987
2. Baker, C. T. H., Bocharov, G. A., Paul, C. A. H.: Mathematical modelling of the Interleukin-2 T-cell system: A comparative study of approaches based on ordinary and delay differential equations. J. theor. Med. **2**, 117–128 (1997)
3. Baker, C. T. H., Paul, C. A. H.: Pitfalls in parameter estimation for delay differential equations. SIAM J. Sci. Comput. **18**, 305–314 (1997)
4. Baker, C. T. H., Paul, C. A. H., Willé, D. R.: Issues in the numerical solution of evolutionary delay differential equations. Adv. Comp. Math. **3**, 171–196 (1995)
5. Baker, M. F. L., Sanger, L. J., Rodgers, R. W., Jabboury, K., Mangini, O. R.: Cell proliferation kinetics of normal and tumour tissue in vitro: Quiescent reproductive cells and the cycling reproductive fraction. Cell Prolif. **28**, 1–15 (1995)
6. Bard, Y.: Nonlinear parameter estimation. New York: Academic Press 1974
7. Bocharov, G. A., Romanyukha, A. A.: Mathematical model of antiviral immune-response-III – Influenza-A virus-infection. J. theor. Biol. **167**, 323–360 (1994)
8. Busenberg, S. A., Cooke, K. L.: Periodic solutions of delay differential equations arising in some models of epidemics. In: Proceedings of applied nonlinear analysis conference, Univ. of Texas, New York: Academic Press 1978

9. Cain, S. J., Chau, P. C.: Transition probability cell cycle model part I – Balanced growth. J. theor. Biol. **185**, 55–67 (1997)
10. Cameron, I. L., Padilla, G. M.: Cell synchrony. Studies in biosynthetic regulation. New York: Academic Press 1966
11. Cantrell, D. A., Smith, K. A.: The Interleukin-2 T-cell system – A new cell-growth model. Science **224**, 1312–1316 (1984)
12. Cantrell, D. A., Smith, K. A.: Transient expression of Interleukin-2 receptors – Consequences for T-cell growth. J. exp. Med. **158**, 1895–1911 (1983)
13. Chiu, C., Hoppensteadt, F. C.: A particle method for population shock waves with application to synchronization of bacterial culture growth. In: Proceedings of first world congress of nonlinear analysts, Tampa, Florida. Berlin: de Gruyter 1992
14. Gong, J., Li, X., Traganos, F., Darzynkiewicz, Z.: Expression of G(1) and G(2) cyclins measured in individual cells by multiparameter flow-cytometry – A new tool in the analysis of the cell-cycle. Cell Prolif. **27**, 357–371 (1994)
15. Hoppensteadt, F., Izhikevich, E.: Weakly connected neural networks. Berlin: Springer-Verlag 1997
16. Jonassen, T. S., Seglen, P. O., Stokke, T.: The fraction of cells in G(1) with bound retinoblastoma protein increases with the duration of the cell-cycle. Cell Prolif. **27**, 95–104 (1994)
17. Kuang, Y.: Delay differential equations with applications in population dynamics. Boston: Academic Press 1993
18. Marchuk, G. I., Petrov, R. V., Romanyukha, A. A., Bocharov, G. A.: Mathematical-model of antiviral immune-response 1. Data-analysis, generalized picture construction and parameter evaluation for Hepatitis-B. J. theor. Biol. **151**, 1–40 (1991)
19. Marusic, M., Bajzer, Z., Freyer, J. P., Vukpavlovic, S.: Analysis of growth of multicellular tumor spheroids by mathematical models. Cell Prolif. **27**, 73–94 (1994)
20. McLean, A. R.: T-memory cells in a model of T-cell memory. In: A. S. Perelson et al.: Theoretical and experimental insights into immunology (NATO ASI series, vol. H66, pp. 149–162) Berlin: Springer-Verlag 1992
21. Metz, J. A. J., Diekmann, O.: The dynamics of physiologically structured populations. Lect. Notes Biomath. Berlin: Springer-Verlag 1986
22. Mitchison, J. M., Vincent, W. S.: A method of making synchronous cell cultures by density gradient centrifugation. In: I.L. Cameron et al.: Cell synchrony. Studies in biosynthetic regulation. New York: Academic Press 1966
23. Morel, B. F., Kalagnanam, J., Morel, P. A.: Mathematical modelling of Th1-Th2 dynamics. In: A. S. Perelson et al.: Theoretical and experimental insights into immunology (NATO ASI series, vol. H66, pp. 171–191) Berlin: Springer-Verlag 1992
24. Moreno, S., Nurse, P.: Regulation of progression through the G1 phase of the cell-cycle by the rum1(+) gene. Nature **367**, 236–242 (1994)
25. Moskophidis, D., Lechner, F., Pircher, H., Zinkernagel, R. M.: Virus persistence in acutely infected immunocompetent mice by exhaustion of antiviral cytotoxic effector T-cells. Nature **362**, 758–761 (1993)
26. Novak, B., Tyson, J. J.: Quantitative analysis of a molecular model of mitotic control in fission yeast. J. theor. Biol. **173**, 283–306 (1995)
27. Oden, J. T., Zohdi, T., Cho, J.-R.: Hierarchical modelling. A posteriori error estimation and adaptive methods in computational mechanics. In: Computational methods in applied sciences (pp. 37–47). New York: Wiley 1996

28. Paul, C. A. H.: A user-guide to Archi – An explicit Runge–Kutta code for solving delay and neutral differential equations and parameter estimation problems. MCCM report **283**, ISSN 1360–1725, University of Manchester 1997
29. Ratkowsky, D. A.: Nonlinear Regression Modeling: A Unified Practical Approach. New York: Marcel Dekker 1983
30. Santisteban, M. S., Brugal, G.: Image-analysis of in-situ cell-cycle related changes of PCNA and KI-67 proliferating antigen expression. Cell Prolif. **27**, 435–453 (1994)
31. Sherley, J. L., Stadler, P. B., Stadler, J. S.: A quantitative method for analysis of mammalian cell proliferation in culture in terms of dividing and non-dividing cells. Cell Prolif. **28**, 137–144 (1995)
32. Sinko, J. W., Streifer, W.: A model for populations reproducing by fission. Ecol. **52**, 330–335 (1971)
33. Smith, H. L.: Reduction of structured population models to threshold-type delay equations and functional differential equations: A case study. Math. Biosci. **113**, 1–23 (1993)
34. Smith, J. A., Martin. L.: Do cells cycle?. Proc. Natl. Acad. Sci. USA **70**, 1263–1267 (1973)
35. Smith, K. A.: Interleukin-2 – Inception, impact and implications. Science **240**, 1169–1176 (1988)
36. Sidorov, I. A., Romanyukha, A. A.: Mathematical modelling of T-cell proliferation. Mathematical Biosciences **115**, 187–232 (1993)
37. Talavera, F., Bergman, C., Pearl, M. L., Connor, P., Roberts, J. A., Menon, K. M. J.: cAMP and PMA enhance the effects of IGF-I in the proliferation of endometrial adenocarcinoma cell line HEC-1-A by acting at the G_1-phase of the cell cycle. Cell Prolif. **28**, 121–136 (1995)
38. Zennaro, M.: Natural continuous extensions of Runge–Kutta methods. Math. Comput. **46**, 119–133 (1986)